Ring patterns in high-current field emission from carbon nanotubes

Mickaël Marchand, Catherine Journet, Christophe Adessi, and Stephen T. Purcell

Laboratoire de Physique de la Matière Condensée et Nanostructures, CNRS, UMR 5586, Domaine Scientifique de la Doua,
Université Lyon 1, F-69622 Villeurbanne Cedex, France

In this paper we explain the origin of the ring structure that sometimes forms a sharp border surrounding field-emission electron microscopy patterns from carbon nanotubes (CNTs) at high current. The rings turn out to be due to the self-focusing of thermal-field electrons emitted from the near-cap shank of a CNT that reaches high temperature through Joule heating. To prove this we have simulated the electrostatic fields, the dependence of electron emission on field, temperature, and position on the CNT, and the emitted electron trajectories for different CNT/electrode geometries. The rings are formed when the manifold of emitted electron trajectories folds over onto itself due to self-focusing by the back-support plane. Sufficient thermal electron currents can only be emitted because CNTs can maintain a continuous high-temperature self-heating state, a state for now unique to carbon nanotubes. We do not need to evoke space charge effects and a program based on Green's functions is to calculate the field emission current for all values of field and temperature. The original observation of this phenomenon goes back to at least the pulsed high current experiments on W emitters in the 1950s [W. P. Dyke, J. K. Trolan, E. E. Martin, and J. P. Barbour, Phys. Rev. **91**, 1043 (1953); W. W. Dolan, W. P. Dyke, and J. K. Trolan, Phys. Rev. **91**, 1054 (1953)] and thus this work resolves a long-standing riddle in field emission.

PACS number(s): 68.37.Vj, 61.46.Fg

I. INTRODUCTION:

Field emission (FE) from carbon nanotubes (CNTs) is one of the most promising domains for nanotubes with many identified applications[1] including flat panel displays, individual high brightness sources for better electron microscopy and e-beam lithography, microguns for miniature scanning electron microscopy, microwave amplifiers, miniature x-ray tubes, lighting, discharge tubes, vacuum gauges, etc. This is because CNTs have several advantages as FE electron sources: chemical stability, high current carrying capacity, high aspect ratios for low extraction voltages, stable emission, small overall size, and low-cost mass production.

Many applied and fundamental studies have been carried out in order to understand the specificity of CNT emitters,[1–4] usually after[5] and even during their growth.[6,7] One particular and noteworthy aspect is that they emit stably in a high-temperatures state (>1600 K) that is induced by self Joule heating in the nanotube itself.[8] This is unlike metal emitters which suddenly explode at higher currents due to catastrophic runaway phenomenon that quickly follows any induced heating.[9,10] To our knowledge there are no measurements in the literature of a stable heating to any increased temperature of a metal emitter. This stable heating has far ranging effects because it allows high current operation, self cleaning by desorption and gradual as opposed to sudden breakdown and it is an essential element of the analysis in this paper.

A particular phenomenon observed during FE at high currents from CNTs is the formation of rings around the central field-emission electron microscopy (FEM) pattern[5,6,11,12] for which the origin has not yet been clearly identified and which is the subject of this paper. Similar patterns were first observed by Dyke *et al.*[9] and studied later by Fursey and Sokol'skaya[13,14] with metal field emitters operating under extreme current densities in pulse mode. These are quite different from the rings observed in FEM images by Saito *et al.*[15] which they attributed to the open section of multiwall nanotubes (MWNTs). Also, circular patterns were also observed[16,17] which were somewhat different from those just mentioned with the less sharp and less round circles.

The authors of the early work on metal emitters argued that the rings were connected to high temperatures induced by resistive heating that enhanced the thermally assisted field emission away from the emitter apex. However no calculations of the ring intensities were provided and the interplay of different possible phenomena: thermal-field emission, space charge, and even surface reconstruction,[18] was not clarified. Batrakov *et al.*[19] re-examined this analysis more recently and showed how rings can be formed by the self-focusing of electrons from the neck region of the specific geometry of thermally formed metal emitters that self heat by Joule effects. As we see below their analysis is similar to ours, however to obtain rings they used unrealistic fields, found it necessary to include space charge effects and did not calculate the full thermal-field tunneling current over the whole emitter surface (see below) which is necessary to have a quantitative analysis of the phenomena. As well they did not treat the case of nanotubes which have a different geometrical shape.

In the case of the CNT rings, Dean *et al.*[5] stated that the intensities of the rings were amplified if the substrate temperature was increased. They then evoked the work on metal tips[9] to suggest that the CNT rings were also due to a thermal heating of the emitters by local Nottingham effects at the tip apex. Similarly, Bonard *et al.*,[6] who also observed rings apparition during growth of carbon nanotubes under field emission with a heated substrate, suggested that the formation of these rings appeared when the temperature was sufficient to reach the intermediate state between field emission and thermoelectronic emission. However, neither of these authors
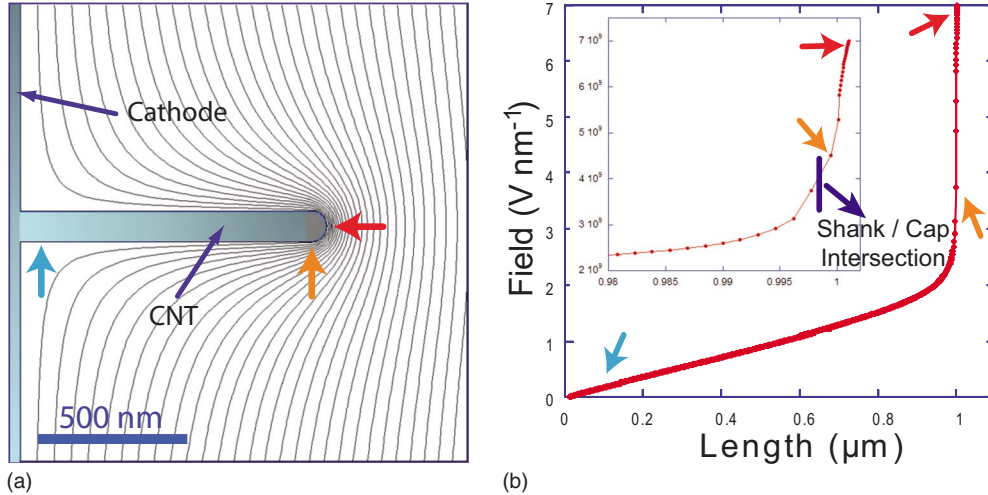
FIG. 1. (Color online) (a) Zoom of the geometry used for the simulations and calculated equipotential lines near a nanotube. (b) Electric field on the surface of the nanotube.

proposed a model of how the rings form, did not identify where the electrons come from and thus did not predict the ring intensity, angular spread, and sharpness. Walker *et al.*[20] has proposed that the rings are due to interactions of the emitted electrons by space charge effects. However their rings are actually disks with small holes in the center and we see below that rings can form without space charge. Another explanation for the rings is that they are formed by the secondary electrons generated at the screen that are reattracted to the surface in the diode configuration.[17] This may explain the somewhat different rings of Refs. 16 and 17 but are unlikely to explain the sharp rings found in experiment and this explanation does not bring in the temperature of the emitter. We have also remarked the formation of quite different circular disks of light surrounding the bright light spots of intense electron fluxes, which we believe are an artifact due to internal reflection of light within the glass support plate.

In this paper, we present a detailed model that explains that the sharp rings are indeed formed by electrons emitted in the thermal-field regime away from apex of hot nanotubes. The nanotubes are assumed to be self heated by Joule effects to temperatures in excess of 1500 K as proven in experiments.[8] Electrons emitted from the near-apex shank are concentrated into rings by the forward focusing of the back-support plane. The simulations are based on calculations of three elements from basic field emission: (1) electrostatic fields and potentials of the CNT geometry in space and, in particular, over the whole CNT surface; (2) the emitted current density at all surface points and at different temperatures corresponding to experimental results. It is not necessary to include simulations of the corresponding heat generation and conduction problem because high temperatures have been found experimentally and previous simulations[21] show that the temperature is relatively uniform over an important part of the free end side of a nanotube which provides practically all the emission. The emitted current density is found with a program based on Green's functions[22] that is capable of calculating the tunneling current even in the intermediate regime between Schottky and field emission; (3) electron trajectories from the CNT to

screen for the observed FE pattern. No space charge effects are necessary and all parameters and geometries are common to actual experiments.

II. EXPERIMENTAL PROCEDURE

We use the charged particle optics (CPO) software[23] which is based on the boundary element method to calculate the potentials, surface charges, and fields everywhere in our system. Our model [see Fig. 1(a)] is composed of a cylindrical emitter closed by a hemisphere that mimics the geometry of a single-wall carbon nanotube (diameter $\phi = 2$ nm, length $L = 1$ μm). The CNT is placed perpendicular on a flat cathode with a negative voltage of 500 V. For the ring formation, a planar extraction anode is situated in front of the nanotube at a distance of 60 μm from the cathode in order to give a field of 0.7 V/Å at the apex. The final trajectories vary only a little for similar CNT dimensions and practically not at all for a constant aspect ratio. Our single-wall nanotube is divided into 675 uniform segments each of which carries an electrical charge on its surface.

With the calculated field profile along the nanotube, $F(x)$, we determine the electron current density $J_E[F(x), T]$ on the whole surface of the nanotube, where T is the temperature. $J_E(F, T)$ was calculated using the program of Adessi *et al.*[22] which resolves the one-body Schrödinger equation using a Green's formalism for F ranging from 0.04 to 0.8 V/Å and T from 300 to 3000 K in steps of 100 K. This program closes the gap between the Richardson/extended Schottky (RS) emission and thermally assisted Fowler Nordhein (TFN) emission regimes, which is crucial for calculating the current in the ring structures. The image charge potential is used. We have controlled that this program gives the same currents as the analytical formula.[24] Another approach would have been to use the extrapolation methods.[25–27] The emitted current I_E is obtained by multiplying $J_E[F(x), T]$ with each segment surface S_E of the emitter.

We simulate the trajectories of the electrons emitted perpendicularly to the surface of each segment of the nanotube
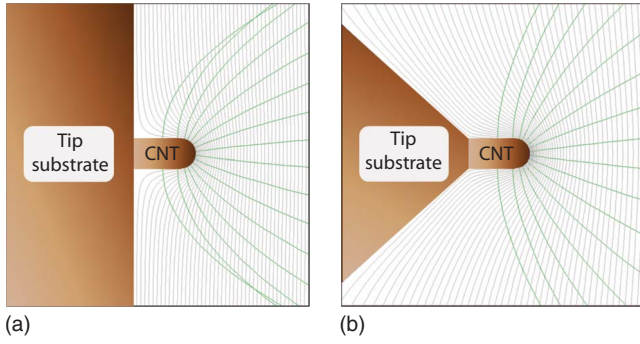
FIG. 2. (Color online) Simulations of the trajectories of electrons from the nanotube to the anode screen for two support geometries: (a) planar and (b) conical. The Y scale is multiplied by 100 times so that one distinguishes the important details of the trajectories. Note that the last two trajectories cross for the planar substrate but not for the cone.

also using the CPO software. The electrons are given a small initial energy $E_k(0)$ without which the program cannot calculate physically sensible trajectories. $E_k(0)$ was varied over 1–2 eV to show that it has little effect on the final emitted patterns. The reader is reminded that in a two potential system, trajectories do not vary with the magnitude of the voltage[28] except for small effects due to initial energies. These trajectories end on the planar anode located 60 μm in front of the nanotube forming circular emission patterns. A current is attributed to each trajectory by the previous calculations. Assuming that the current is conserved, the current density on the anode J_A is deduced from the relation: $J_A = J_E \times S_E / S_A$, where S_A is the surface area of the disk between two successive electron trajectories arriving on the anode.

III. RESULTS

Figure 1(a) shows the form of the potential around the nanotube and Fig. 1(b) shows the field profile along the length of the nanotube. This is the general form of the field
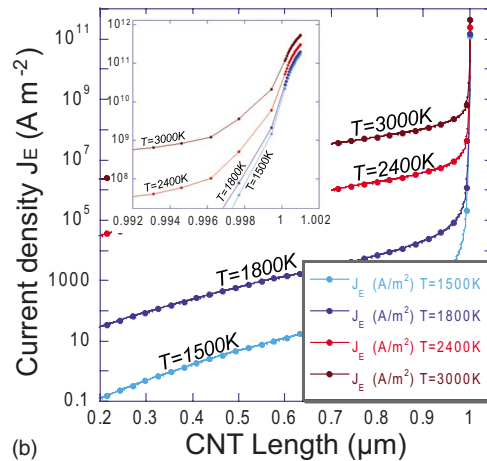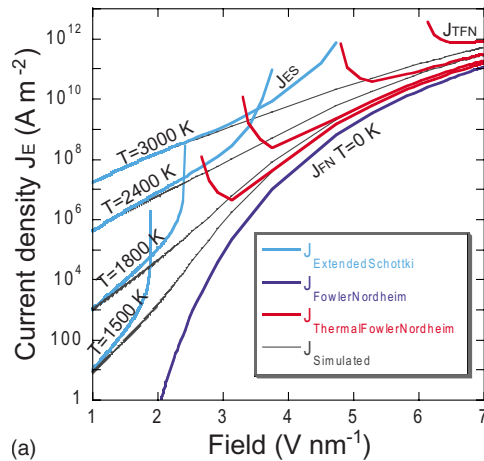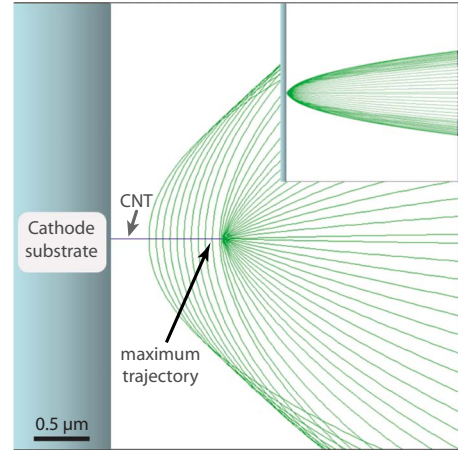

FIG. 3. (Color online) Larger scale views of an envelope of simulated trajectories showing the concentration near the extremity of the pattern.

for any long cylindrical emitter vertical to a plane. The field follows a fairly linear increase starting from the base until it suddenly starts to peak near the cap, reaching the chosen value of 0.7 V/Å at the apex. The field at the cap/shank junction is ~1/3 the maximum value at the apex [see inset Fig. 1(b)].

In Fig. 2(a) we show a selection of simulated trajectories from one more complete series. At a certain position on the nanotube the corresponding trajectories fold over onto each other creating a singularity in the intensity at the screen. This is the origin of the ring phenomena for nanotubes. However we must still show that there is sufficient intensity in the rings for reasonable experimental emission conditions (see below). In Fig. 2(b) we show simulations for a nanotube that terminates a cone tip. In this case there is no folding over of the trajectories. This shows that the rings are strongly influenced by the support structure. Figure 3 is a larger view of the trajectory envelope that shows that a large number of paths concentrate to a particular place on the anode screen for a flat back electrode.

Figure 4(a) presents the $J_E(F,T)$ versus the F for four

(a)

(b)

FIG. 4. (Color online) (a) $J_E(F,T)$ versus F for different chosen temperatures. The dotted lines are the simulated by the exact calculation. (b) $J_E(x,T)$ along the nanotube.
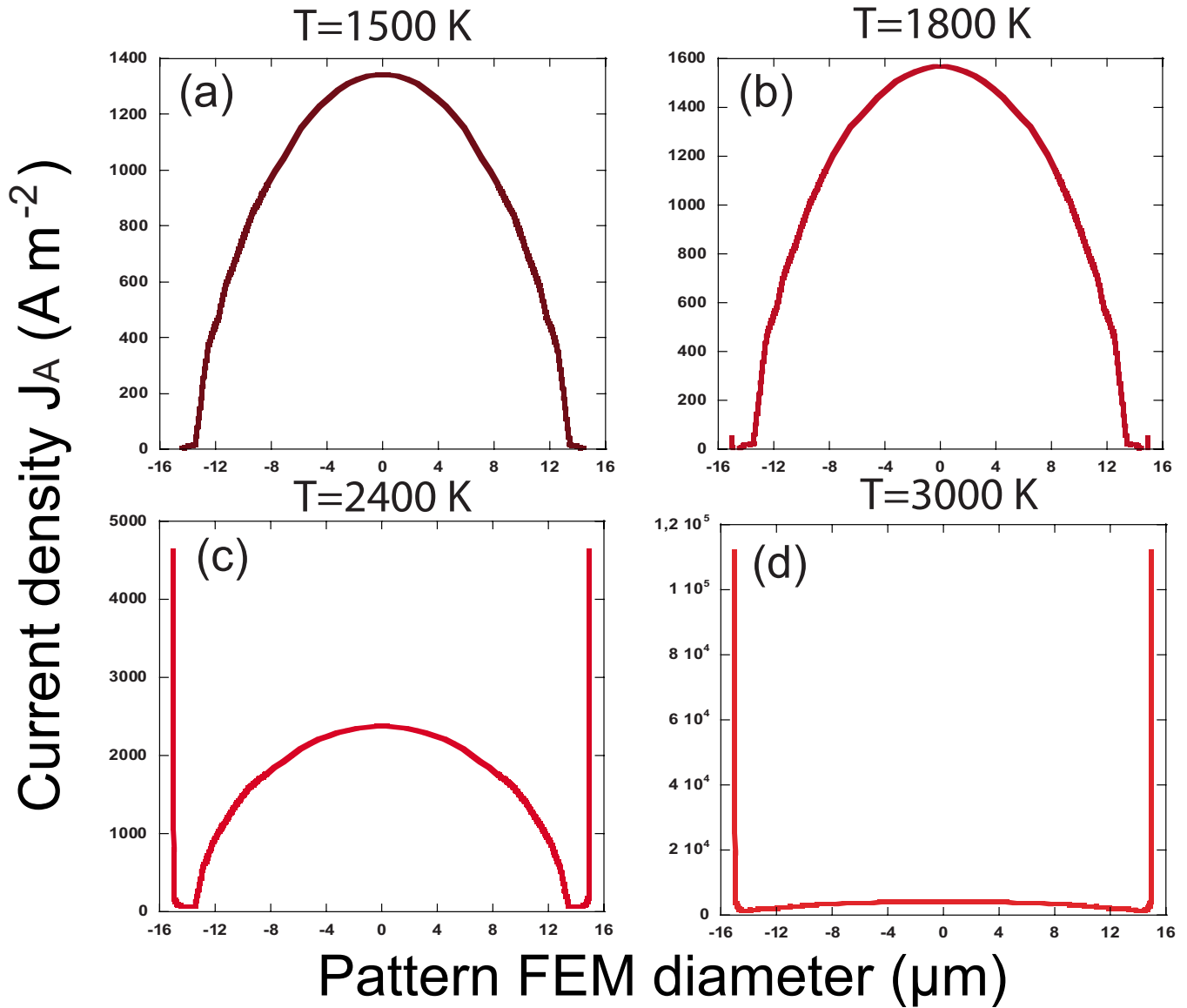
FIG. 5. (Color online) Calculated current densities as a function at a node screen as a function of distance from the center.

different temperatures. Calculations from the analytical formulas for the two conventional emission regimes of high-temperature low field and low-temperature high field are also represented in the plot. We obtain results without any kinks due to approximations, which is important because these are the electrons that form the rings. Otherwise even an approximate quantitative agreement between the theoretical calculations and experiments is difficult. It is clear in Fig. 4(a) that the current density in the RS zone is strongly dependent on the temperature while in the TFN zone it depends more on field variations. The TFN equation is valid for a zone from the apex to 0.2% of the nanotube length (2 nm) for a temperature of 3000 K and to 0.4% for $T=1500$ K (4 nm). The RS equation describes the behavior of the current density from the bottom of the nanotube to 0.98 μm of its length (20 nm from the cap) for $T=3000$ K and 0.56 μm for $T=1500$ K. We plot the current density as a function of position along the tip for different temperatures [Fig. 4(b)]. These curves are very well peaked at the CNT's cap where

the current density is more sensitive to the field than to the temperature. The effect of the temperature on the current density is more visible along the CNT length and gives non-negligible current density at a certain distance from the cap which is sufficient to create the rings through the self-focusing effect.

The $J_E(x, T)$ profile along the length of the nanotube is combined with the electron trajectories to give the electron-density profile on the anode situated in front of the nanotube. Figure 5 shows two-dimensional (2D) profiles of the electron density versus the arrival position of the electrons on the anode for the four studied temperatures. The zero of the X axis corresponds to the axis of the nanotube. On Fig. 5(c), it is clearly seen the apparition of peaks situated at 14.7 μm. These peaks appear for $T \geq 1800$ K and their intensity is higher than that of the central circular field-emission pattern for temperatures above $T > 2300$ K. With this 2D profile, we can reconstruct a field pattern image giving the current density on the anode for the four temperatures (Fig. 6). One sees
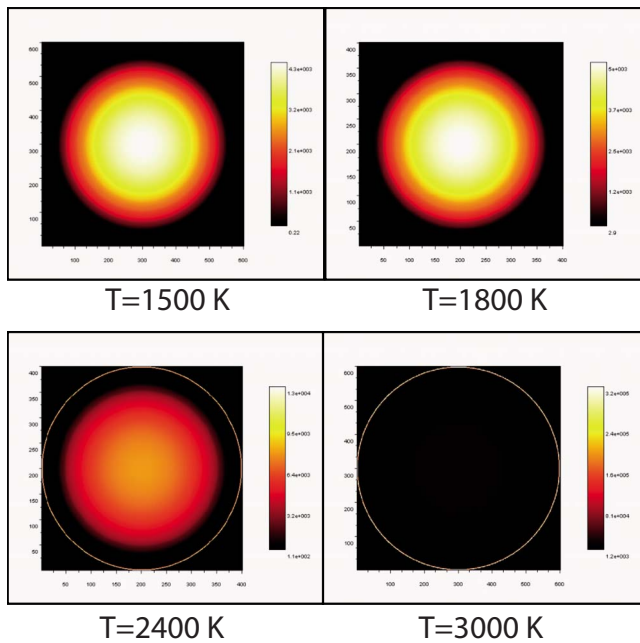
FIG. 6. (Color online) 2D reconstruction of the emission pattern. The bright rings are visible at about 1800 K and dominate above 2400 K.

that these images give rings whose intensities depend strongly on the temperature.

IV. DISCUSSION

Now that the source of the rings is established several finer points are worth discussing. The intensity of rings are directly connected to the temperature and thus, in principle, they provide an alternative method for studying heating effects and thermal-field emission in a quantitative way. A potential problem is that the temperatures used here are ~20% higher than the only estimate in the literature by Dean, *et al.*[11] of ~1600 K for the minimum temperature for observing the ring patterns. As well we found severe degradation of CVD MWNTs when they reached 2000 K by Joule heating.[8] The simulations require ~2000 K for equal intensity of rings and direct emission and even higher for dominating rings. This is not a severe contradiction but several factors worth discussing may come into play. (Note that varying the work function for carbon over the range found in the literature has little influence.) First, it is known that the current

density calculated by free electron FN theory with image charge and thermal effects is still a factor of five different from the best quantitative measurements.[29] This difference is proposed to be due to the deficiency of the classical image charge model to describe correctly the tunneling barrier. It is therefore highly probable that the ratio of intermediate emission to thermal-field emission calculated here, which determines the relative ring intensity, does not describe well the experiment because the electrons pass through different heights of the surface barrier. A second point is that our calculations are for the total current emitted and they assume perfect vertical emission from the surfaces. Electron emission has tangential components that increase proportionally as the temperature is raised, for example, blurring the FE patterns. This tends to push emission off axis and therefore would reinforce the ring intensities. Simulating this is obviously an extra step of complexity. Third, the cap apex may be cooler than the near-cap shank first because of Nottingham effects and second due to loss of current before it reaches the apex by thermal-field emission. Finally it is not obvious that the temperature measurements are very precise. In view of this discussion, the discrepancy between the measurements and our simulations is not surprising.

Our simulations give very sharp, individual rings while wider[5,6] and sometimes multiple concentric rings are described in the literature. Both the tangential emission and a variable initial energy will blur the rings. Multiple rings may be caused by local hot spots further down the nanotube shank that can occur at defects sites that have higher electrical resistances. These may generate concentrate rings inside the original one.

V. CONCLUSION

The electrostatic fields, electron trajectories, and position-dependent emission currents on which our simulation of the rings are all based on standard field-emission principles and the assumed temperatures are in the range of those found in experiment. Thus our explanation of the formation of the rings is as sure as these principles. We do not need to evoke space charge for effects as in Ref. 20. In any case the rings were observed for μA currents[11] while classically space charge effects are found for FE tip emitters approaching the mA range.[30] A very interesting experiment that would corroborate our results would be to measure the energy distributions across the emission patterns including the ring structures.

[1] See for, e.g., N. de Jonge and J.-M. Bonard, Philos. Trans. R. Soc. London, Ser. A **362**, 2239 (2004).

[2] D. Lovall, M. Buss, E. Graugnard, R. P. Andres, and R. Reifenberger, Phys. Rev. B **61**, 5683 (2000).

[3] M. J. Fransen, T. L. van Rooy, and P. Kruit, Appl. Surf. Sci. **146**, 312 (1999).

[4] J.-M. Bonard, H. Kind, T. Stöckli, and L.-O. Nilsson, Solid-State Electron. **45**, 893 (2001).

[5] K. A. Dean, P. von Allmen, and B. R. Chalamala, J. Vac. Sci. Technol. B **17**, 1959 (1999).

[6] J.-M. Bonard, M. Croci, F. Conus, T. Stöckli, and A. Chatelain, Appl. Phys. Lett. **81**, 2836 (2002).

[7] M. Marchand, C. Journet, D. Guillot, J.-M. Benoit, B. I. Yakobson, and S. T. Purcell, Nano Lett. **9**, 2961 (2009).

[8] S. T. Purcell, P. Vincent, C. Journet, and V. Thien Binh, Phys. Rev. Lett. **88**, 105502 (2002).

[9] W. P. Dyke, J. K. Trolan, E. E. Martin, and J. P. Barbour, Phys. Rev. **91**, 1043 (1953).

[10] W. W. Dolan, W. P. Dyke, and J. K. Trolan, Phys. Rev. **91**, 1054 (1953).

[11] K. A. Dean, T. P. Burgin, and B. R. Chalamala, Appl. Phys. Lett. **79**, 1873 (2001).

[12] J.-M. Bonard, M. Croci, C. Klinke, F. Conus, I. Arfaoui, T. Stöckli, and A. Chatelain, Phys. Rev. B **67**, 085412 (2003).

[13] I. L. Sokol'skaya and G. N. Fursey, Radiotekh. Elektron. (Moscow) **7**, 1474 (1962).

[14] I. L. Sokol'skaya and G. N. Fursey, Radiotekh. Elektron. (Moscow) **7**, 1484 (1962).

[15] Y. Saito, K. Hamaguchi, K. Hata, K. Uchida, Y. Tasaka, F. Ikazaki, M. Yumura, A. Kasuya, and Y. Nishina, Nature (London) **389**, 554 (1997).

[16] W. Zhu, C. Bower, O. Zhou, G. P. Kochanski, and S. Jin, Appl. Phys. Lett. **75**, 873 (1999).

[17] K. N. Nikolski, A. S. Baturin, A. I. Knyazev, R. G. Tchesov, and E. P. Sheshin, Tech. Phys. **49**, 250 (2004).

[18] V. M. Zhukov and N. V. Egorov, Zh. Tekh. Fiz. **61**, 170 (1991).

[19] A. V. Batrakov and D. I. Proskurovskii, Tech. Phys. Lett. **25**, 444 (1999).

[20] D. G. Walker, W. Zhang, and T. S. Fisher, J. Vac. Sci. Technol. B **22**, 1101 (2004).

[21] P. Vincent, S. T. Purcell, C. Journet, and V. T. Binh, Phys. Rev. B **66**, 075406 (2002).

[22] Ch. Adessi and M. Devel, Ultramicroscopy **85**, 215 (2000).

[23] CPO Ltd. charged particle optics programs, cpo@electronoptics.com

[24] See, e.g., L. W. Swanson and A. E. Bell, in *Advances in Electronics and Electron Physics*, edited by L. Marton (Academic, New York, 1973), Vol. 32.

[25] S. G. Christov, Phys. Status Solidi **17**, 11 (1966).

[26] K. L. Jensen and M. Cahay, Appl. Phys. Lett. **88**, 154105 (2006).

[27] M. Dionne, S. Coulombe, and J.-L. Meunier, J. Phys. D **41**, 245304 (2008).

[28] M. K. Miller and G. D. W. Smith, *Atom Probe Microanalysis* (Materials Research Society, Pittsburgh, 1989), p. 26.

[29] C. D. Ehrlich and E. W. Plummer, Phys. Rev. B **18**, 3767 (1978).

[30] W. P. Dyke and W. W. Dolan, in *Advances in Electronics and Electron Physics*, edited by L. Marton (Academic, New York, 1956), Vol. 8, p. 89.